Published in final edited form as:
Environ Sci Technol. 2007 July 15; 41(14): 5137–5142.

Synthesis of plant-mediated gold nanoparticles and catalytic role of biomatrix-embedded nanomaterials

Nilesh C. Sharma[1], **Shivendra V. Sahi**[1], **Sudip Nath**[2], **Jason G. Parsons**[3], **Jorge L. Gardea-Torresdey**[3], and **Tarasankar Pal**[2]

1 *Department of Biology, Western Kentucky University, 1906 College Heights Blvd. # 11080, Bowling Green, KY 42101, USA*

2 *Department of Chemistry, Indian Institute of Technology, Kharagpur 721302, West Bengal, India*

3 *Department of Chemistry, The University of Texas at El Paso, 500 West University Avenue, El Paso, TX 79968-05, USA*

Abstract

Growth of *Sesbania* seedlings in chloroaurate solution resulted in the accumulation of gold with the formation of stable gold nanoparticles in plant tissues. Transmission electron microscopy revealed the intracellular distribution of monodisperse nanospheres, possibly due to reduction of the metal ions by secondary metabolites present in cells. X-ray absorption near-edge structure and extended X-ray absorption fine structure demonstrated a high degree of efficiency for the biotransformation of Au(III) into Au(0) by plant tissues. The catalytic function of the nanoparticle-rich biomass was substantiated by the reduction of aqueous 4-nitrophenol (4-NP). This is the first report of gold nanoparticle-bearing biomatrix directly reducing a toxic pollutant, 4-NP.

Introduction

The field of nanotechnology has recently witnessed spectacular advances in the methods of nanomaterial fabrication and utilizing their exotic physicochemical and optoelectronic properties (1). With the development of new chemical or physical methods, the concern for environmental contaminations is also heightened as the chemical procedures involved in the synthesis of nanomaterials generate a large amount of hazardous byproducts. Thus, there is a need for ‘green chemistry’ that includes a clean, nontoxic and environment-friendly method of nanoparticle synthesis (2). As an alternative to conventional methods, biological methods are considered safe and ecologically sound for the nanomaterial fabrication (1).

Some well-known examples of microbial systems synthesizing inorganic materials include magnetotactic bacteria for magnetite nanoparticles (3,4), S-layer bacteria for gypsum and calcium carbonate layers (5) and silver mine- inhabiting *Pseudomonas* sp. that reduces silver ions to form silver nanoparticles (6). Nanocrystals of gold, silver and their alloys have been synthesized within the cells of lactic acid bacteria (7). Fungus and actinomycete species were reported to synthesize silver or gold nanoparticles of different shapes and sizes (2,8), but use of green plants for similar nanoparticle biosynthesis methodologies is an exciting possibility that is largely unexplored.

The first report of plants synthesizing gold or silver nanoparticles appeared when alfalfa seedlings were shown to uptake gold or silver from metals-enriched nutrient media (9,10).

Correspondence to: Shivendra V. Sahi.

These studies demonstrated that Au(III) or Ag(I) ions were reduced in the solid media to Au (0) or Ag(0) by alfalfa plants, and then the metal atoms were absorbed into the plant, where growth of nanoparticles took place. Another dimension was added to the 'green chemistry' approach for pure metal synthesis with the use of plant broths (1,11). Shankar et al. used lemongrass and geranium plant extracts to induce the formation of gold nanoparticles or structures when reacted with aqueous chloroauric acid (1,11). Here we demonstrate uptake of high amounts of gold(III) ions by a leguminous shrub, *Sesbania drummondii*, with subsequent reduction of Au(III) ions to Au(0) inside plant cells or tissues. What makes our report different from other studies is the intracellular formation and growth of spherical gold nanoparticles (6–20 nm) and their *in situ* catalytic function. The nanoparticle-bearing biomatrix of *Sesbania* has the ability to reduce a hazardous and toxic pollutant, aqueous 4-nitrophenol.

The optoelectronic and physicochemical properties of nanoscale materials are a strong function of particle size. Nanoparticle shape also contributes significantly to modulating their electronic properties (1). Therefore, producing biologically-inspired nanostructures of a desirable size and morphology is critical to their commercial applicability. The shape and size of biogenic nanoparticles depends on the biological species involved, for example, geranium leaf broth reacted with aqueous chloroaurate ions induced a variety of gold nanoparticle shapes that included rods, flat sheets and triangles, while its endophytic fungus (*Colletotrichum* sp.) produced essentially spherical nanoparticles under the same conditions (12). Yet another plant, lemongrass (leaf broth) induced the formation of a high percentage of single-crystalline gold nanotriangles under similar conditions (1). Even the parts of a plant species affect the nature of nanoparticle synthesis. The root broth prepared from geranium exhibited a propensity towards forming flat nanostructures in comparison with the spherical nanoparticles that formed with geranium stem broth (11).

Experimental Section

In vitro growth of seedlings in gold solution

Seeds of Sesbania drummondii were scarified in 85% H_2SO_4 for 40 min, rinsed for 30 min; sterilized in 0.1% $HgCl_2$ followed by rinsing (3-times) with sterile deionized water. Seeds were then plated on sterile agar-water medium in Magenta box and germinated in growth chamber (25–28°C; dark for 4 d followed by 16/8 h of light and dark cycle). Aseptically germinated 3-week-old seedlings (8–10 cm long shoots and 4–6 cm long roots) were transferred individually to flasks (200 ml), containing 75 ml sterile deionized water and 0–200 $mg.L^{-1}$ potassium tetrachloroaurate (pH adjusted to 4.8). Flasks were capped with aluminum foil allowing the seedling top to pass through. Seedlings were grown in the growth chamber at 25 ± 2°C; 16 h light and 8 h dark regimen of cool fluorescent light for 6 d. (13). Controls were set up with 0 $mg.L^{-1}$ potassium tetrachloroaurate. In another experiment, seedlings were grown, as above, in sterile deionized water containing 100 $mg.L^{-1}$ potassium tetrachloroaurate for a period of 0–6 d. For this experiment, controls were set up with negligible exposure to 100 $mg.L^{-1}$ potassium tetrachloroaurate. For each treatment, four flasks were maintained as replicates and the experiment was repeated twice. Plants were harvested; separated shoots and roots were washed in detergent solution followed by rinsing several times in sterile deionized water.

Growth measurement

Roots and shoots of randomly chosen identical seedlings (four) were measured (cm) before start of the experiment. Roots and shoots from each treatment were again measured after harvest (6d). The difference in the final and initial length (cm) was calculated as the growth of seedlings. The data were analyzed by two-way analysis of variance where F ratios were significant ($P < 0.05$), using SYSTAT (Version 9 for Windows, 1999, Systat Software Inc., Richmond, CA).

Analysis of gold in plant tissue

Root and shoot samples were weighed and placed in a 15mL screw capped Teflon beaker. Three mL concentrated HNO_3 was added to the sample and beaker was placed on a hot plate at a temperature of 100°C overnight, and then evaporated to dryness. Samples were allowed to cool and made up gravimetrically with 2% HNO_3 to a volume of 20mL. The ICP-MS analysis was carried out using external calibration procedure and Y (0.1 ppm) was used as an internal standard to correct for drift and matrix effect (13).

Transmission electron microscopy

After thorough rinsing of treated plants, roots were cut into pieces at room temperature in 2% glutaraldehyde in 50mM Piperazine-N,N′-bis(2-ethanesulfonic acid) (pH 6.8). These pieces were briefly placed in vacuum to aid infiltration of the fixative into the tissues, and incubated in the fixative for 2 h at room temperature. The samples were then washed in 50mM Piperazine-N,N ′-bis(2-ethanesulfonic acid) buffer, and post-fixed in 2% Osmium tetraoxide in water for 2 h at room temperature. After washing in water, the samples were dehydrated through an ethanol series, and embedded in Spurr's resin (13). Thin sections were prepared by a RMC MT-X ultramicrotome (Boeckeler Instruments, Inc., Tucson, AZ, USA) collected on Cu-support grids, and observed with a 120 CX Transmission electron microscope (JEOL USA, Inc., MA, USA) at 80 kV. Element analysis was carried out at 40 kV using Energy Dispersive X-ray Spectrometer (IXRF Systems Inc., TX, USA). Several treated plant samples were examined and the sample showing the best image was chosen for photographic representation.

X-ray absorption near-edge structure (XANES) and extended X-ray absorption fine structure (EXAFS) analysis

For these analyses, root and shoot pieces were lyophilized using a Labconco freeze-dry system (14). The lyophilized samples were ground using a mortar and pestle to obtain a homogenous mixture and packed into 1.0 mm thick aluminum sample holders with Kapton Tape windows. The samples were run at room temperature using beamline 2–3 at Stanford Synchrotron Radiation Laboratory (Stanford University, Menlo Park, CA, USA). The operating conditions of the beam line were set as follows: energy, 2.0 GeV; current, 80–100 mA; a silicon double crystal monochromator (111 ϕ 0) with a 1.0 mm slit. Model compounds were diluted using boron nitride to give a change of one absorption unit across the absorption edge. All spectra were calibrated against the edge position of a gold foil (11.918 keV). The samples were analyzed using the standard data reduction process and the WinXAS© software (15). After normalization, the XANES spectra were extracted from the spectra by sectioning the XAS spectra to 12.05 keV. The XANES spectra were then fitted to the XANES spectra of model compounds using a linear-combination XANES fitting (10). EXAFS spectra of plant and bulk gold samples were analyzed as in previous studies (19,16)

Catalytic function

In order to study the catalytic function of biomatrix-gold nanomaterials, plant samples carrying gold nanoparticles were cryoground in liquid nitrogen and added to the 4-NP solution. Following sonication, the decolorization was quantitatively monitored using a spectrophotometer (17).

Results and Discussion

Sesbania demonstrated an increased uptake of gold from solutions depending on the concentration of tetrachloroaurate ($KAuCl_4$) in a solution (Figure 1A). Gold concentration in shoots varied from 5–98 $mg.Kg^{-1}$ (DW) at different concentrations of $KAuCl_4$ in the solution (Figure 1A). Gold concentrations in roots varied from 1–9 $g.Kg^{-1}$ depending on the

concentration (25–200 mg.L^{-1}) of $KAuCl_4$ in solutions. The enormous concentration of Au in roots may be partly because of an accelerated uptake and partly because of nanoparticle synthesis at the root surface tissue. It was interesting to note that the color of plant roots changed to light purplish in a week. The color shift is itself an indication of nanoparticle distribution on the root surface. To test further whether plants actively uptake Au, a time course study was designed. The shoot concentrations of Au increased (10–85 mg.Kg^{-1}) over time when seedlings were grown at 100 mg.L^{-1} $KAuCl_4$ (Figure 1B). Alfalfa was shown to absorb gold (0) from media and cause growth of nanoparticles in the tissue, but gold uptake was not quantified (9). In an earlier study, *Brassica juncea* was induced to hyperaccumulate gold (57 mg.Kg^{-1} DW) in the presence of ammonium thiocyanate (18). The growth of *Sesbania* seedlings in gold solution was also studied, and it was observed that the difference in shoot growth of the experimental plants and controls was not significant until the gold concentration in solution reached to a level of 200 ppm, at which shoot growth was affected (Table 1).

Transmission electron microscopy (TEM) revealed a pattern of uniform distribution of gold particles inside plant cells at low magnification (Figure 2A). However, at high magnification, the organellar regions were observed heavily populated with particles. The presence of multiple spherical gold particles surrounding cell organelles in the cytoplasm (Figure 2B) was of special interest. The dense particles dispersed in plant cells were confirmed randomly as gold nanoparticles (Figure 2B inset spectra) by energy-dispersive X-ray spectroscopy. The cellular nanoparticles ranged in 6–20 nm sizes (Figure 2B).

The active uptake of heavy metals has been reported in few wild plants (19). In *Sesbania drummondii*, it has been earlier reported that this plant accumulates lead (Pb) by symplastic mode of transport (13,14). The occurrence of gold nanoparticle, arranged in a definite order, exclusively in the cytoplasm under TEM examination of several root cells (Figure 2B) is indicative of the symplastic transport of gold in this study. We hypothesize that the roots of this plant traps gold from solution as a result of the affinity between carboxylic acid moieties present in the cell wall and Au(III) as reported in other living systems (2). Once gold enters root cells, it is transported symplastically to the conducting tissues and aerial parts of the plants in the manner similar to Pb. With regard to the precise location where synthesis of nanoparticles could occur, the cell wall (external boundary) or cytoplasmic membrane (inner boundary) was demonstrated as the possible site in *Verticillium* sp. (2), whereas periplasmic space was the site for silver nanoparticles assembly in silver-resistant bacteria (6). *Sesbania* thus presents a unique feature of intracellular formation of nanomaterials. The cellular microenvironment is characteristic of a living organism and may impose conditions suitable for uncommon functions such as accumulation and biotransformation of unique elements. The monodispersity, size distribution or the uniformly spherical shape of gold nanoparticles formed inside *Sesbania* cells may be one of such functions.

Transmission electron microscopy evidences the presence of intracellular nanoparticles in *Sesbania*, however, it is important to discern the biotransformation efficiency (the rate of nanoparticle conversion from the total amount of gold in tissues) of a biological system. Therefore, X-ray absorption spectroscopic techniques such as x-ray absorption near-edge structure (XANES) and extended x-ray absorption fine structure (EXAFS) were used in this study to confirm the oxidation state and form of gold in the plant tissue. Figure 3A shows the XANES spectra of the gold model compounds: gold(III) acetate, gold(I) hydroxide, gold sulfide, potassium tetrachloroaurate, and a 1 μm gold metal foil. Figure 3B exhibits the XANES spectra of the gold-laden root and shoot samples. The edge energy or position of the plant samples matches with that of the gold(0) (11.981 keV) foil, and not with that of the initial reactant: tetrachloroaurate. The position of the edge energy clearly shows that the gold present in the plant tissues is gold(0). LC-XANES fittings indicate that 80–85% of gold present in plant samples is constituted of gold(0), and the remaining 15–20% of gold present in plant

tissues is gold sulfide (Table 2). Our results are compatible to the earlier studies using alfalfa plants in respect of XANES spectra (9) but unique in LC-XANES features. LC-XANES fittings have been used to identify the different species of metals present in plants with a high degree of certainty (9, 14).

EXAFS spectra of plant and bulk gold samples were analyzed in this study. As evident from Figure 4, the EXAFS oscillations of gold(0) and plant samples align very well indicating that the majority gold is present as gold(0) in plant samples. As observed in Table 3, the gold(0) foil has 12 neighboring gold atoms at an interatomic distance of 2.86 Å, whereas the plant samples have approximately, 8.6 and 9.8 neighboring gold atoms at a distance of 2.85 Å for the two gold-laden sample. The presence of gold neighbors in the EXAFS is another confirmation for the presence of gold(0) in the plant samples.

It is important to understand the biosynthetic pathway involved in the fabrication of metal nanomaterial mediated by a biological system to gain a better control on the process and products. Little is known so far about the interaction of biomolecules and gold nanoparticles. Shankar et al. (1) believed that the reduction of tetrachloroaurate ions was caused by the reducing sugar present in the lemongrass extract, while the growth of gold nanotriangle crystal was the result of an interaction between *de novo* gold nanoparticles and aldehydes/ketones present in the extract. The reduction of the metal ions and stabilization of the gold/silver nanoparticles was believed to occur by the various terpenoids or alkaloids present in the geranium extract (11). Similarly, *S. drummondii*, used in this study, has been reported for its contents of alkaloids or other secondary metabolites (20) that might function as a reducing agent for the reduction of gold ions and stabilization of nanoparticles in cells. Identification and isolation of the biomolecules responsible for the fabrication of observed monodisperse nanoparticles is currently in progress.

The catalytic function of biomatrix-gold nanomaterial was substantiated by carrying out the reduction of a hazardous and toxic pollutant- aqueous 4-nitrophenol (4-NP), which has a peak at 317 nm in the UV-visible spectral range (Figure 5A). Addition of sodium borohydride to the 4-NP immediately results in a shift in the peak to 400 nm with intensification of color of the solution (Figure 5B). In the absence of any catalyst, the peak at 400 nm remained unaltered even for 2d. Plant samples carrying gold nanoparticles were cryoground in liquid nitrogen and added to the 4-NP solution. Following sonication, the crushed biomatrix- nanomaterial induced fading of the characteristic yellow color of the 4-NP solution on incubation. The decolorization was quantitatively monitored using a spectrophotometer, and a successive decrease in the peak intensity was observed over time (Figure 5B). The decrease in peak arises as a result of the adsorption of 4-nitrophenolate ions by the crushed nanomaterials, which finally produce a colorless solution at the end. When sodium borohydride was added to the colorless solution, it showed a new peak at ~290 nm (Figure 5B) because of the reduction of 4-nitrophenolate species to 4-aminophenol (4-AP) (17). A control experiment with roots devoid of gold nanoparticles did not give any signature of 4-AP under the same experimental condition (Figure 5C). In that case, only the decrease in the absorbance of 4-NP peak was observed as a consequence of the adsorption of nitrophenolate ions by the solid mass. The generation of 4-AP (Figure 5B) confirms the catalytic activity of the gold nanoparticles for the reduction of 4-NP in aqueous solution (17). This observation authenticates the presence and surface activity of gold nanoparticles in the biomatrix. The exploitation of the *in situ* generated gold nanoparticles for a catalytic reaction is a definite departure from the conventional methods, where separation of nanoparticles from a biological system has been a difficult task.

In conclusion, this study demonstrates an interesting case of plant-mediated gold nanoparticle synthesis, and *in situ* catalytic functions of the nanoparticle-rich biomatrix. The reduction of metal ions occurs in the root cells resulting in the formation of nanoparticles that are transported

symplastically to the aerial parts or shoots. The biomatrix nanomaterial exhibited fairly well-defined dimensions and monodispersity. This is a novel introduction of a cell-immobilized stable catalyst which may find applications in future.

Acknowledgements

The authors acknowledge the financial support from the Applied Research and Technology Program and Faculty Scholarship Grant from Western Kentucky University. Thanks are also due to Dr. John Andersland and Adam H. Small for their valuable help with electron microscopy. J. Gardea-Torresdey acknowledges the support from National Institute of Health (grant S06 GM8012-33) and the University of Texas at El Paso's Center for Environmental Resource Management through funding from the US EPA-Office of Exploratory Research. The financial support from NIEHS (grant R01ES11367-01), the Southwest Center for Environmental Research and Policy program, and the HBCU/MI, Environmental Technology Consortium (funded by the Department of Energy) is greatly acknowledged. Portions of this research were carried out at the Stanford Synchrotron Radiation Laboratory, Stanford University on behalf of U.S. Department of Energy.

References

1. Shankar SS, Rai A, Ankamwar B, Singh A, Ahmad A, Sastry M. Biological synthesis of triangular gold nanoprisms. Nature Materials 2004;3:482–488.
2. Mukherjee P, Ahmad A, Mandal D, Senapati S, Sainkar SR, Khan MI, Parishcha R, Ajaykumar PV, Alam M, Kumar R, Sastry M. Fungus-mediated synthesis of silver nanoparticles and their immobilization in the mycelial matrix: a novel biological approach to nanoparticle synthesis. Nano Lett 2001;1:515–519.
3. Spring H, Schleifer KH. *System*. Diversity of magnetotactic bacteria. Appl Micribiol 1995;18:147–153.
4. Dickson DPE. Nanostructured magnetism in living systems - condens. Matter. J Magn Magn Mater 1999;203:46–49.
5. Pum D, Sleytr UB. The application of bacterial S-layers in molecular nanotechnology. Trends Biotechnol 1999;17:8–12.
6. Joerger R, Klaus T, Granqvist CG. Biologically produced silver-carbon composite materials for optically functional thin-film coatings. Adv Mater 2000;12:407–409.
7. Nair B, Pradeep T. Coalescence of nanoclusters and formation of submicron crystallites assisted by *Lactobacillus* strains. Crystal Growth Des 2002;2:293–298.
8. Ahmad A, Senapati S, Khan MI, Kumar R, Sastry M. Extracellular biosynthesis of monodisperse gold nanoparticles by a novel extremophilic actinomycete, *Thermomonospora* sp Langmuir. 2003;19:3550–3553.
9. Gardea-Torresdey JL, Parsons JG, Gomez E, Peralta-Videa J, Troiani HE, Santiago P, Jose Yacaman M. Formation and growth of Au nanoparticles inside live alfalfa plants. Nano Lett 2002;2:397–401.
10. Gardea-Torresdey L, Gomez E, Peralta-Videa JR, Parsons JG, Troiani H, Jose Yacaman M. Alfalfa spouts: a natural source for the synthesis of silver nanoparticles. Langmuir 2003;19:1357– 1361.
11. Shankar SS, Rai A, Ahmad A, Sastry M. Biosynthesis of silver and gold nanoparticles from extracts of different parts of the geranium plant. App Nano Sci 2004;1:69–77.
12. Shankar SS, Ahmad A, Pasricha R, Sastry M. Bioreduction of chloroaurate ions by geranium leaves and its endophytic fungus yields gold nanoparticles of different shapes. J Mater Chem 2003;13:1822–1826.
13. Sahi SV, Bryant NL, Sharma NC, Singh SR. Characterization of a lead hyperaccumulator shrub, *Sesbania drummondii*. Environ Sci Technol 2002;36:4676– 4680. [PubMed: 12433181]
14. Sharma NC, Gardea-Torresdey JL, Parsons J, Sahi SV. Chemical speciation and cellular deposition of lead in *Sesbania drummondii*. Environ Toxicol Chem 2004;23:2068– 2073. [PubMed: 15378980]
15. Ressler T. *J. WinXAS*: a program for X-ray absorption spectroscopy data analysis under MS-Windows. Synchrotron Radiat 1998;5:118–122.
16. Ravel B. *J. ATOMS*: crystallography for the X-ray absorption spectroscopist. Synchrotron Radiat 2001;8:314–316.

17. Praharaj S, Nath S, Ghosh SK, Kundu S, Pal T. Immobilization and recovery of Au nanoparticles from anion exchange resin: resin-bound nanoparticle matrix as a catalyst for the reduction of 4-nitrophenol. Langmuir 2004;20:9889–9892. [PubMed: 15518467]

18. Anderson CWN, Brooks RR, Stewart RB, Simcock R. Harvesting a crop of gold in plants. Nature 1998;395:553–554.

19. Brooks, RR. Plants that Hyperaccumulate Heavy Metals: their Role in Phytoremediation, Microbiology, Archaeology, Mineral Exploration and Phytomining. Cab International; Wallingford, UK: 1998.

20. Powell RG, Smith CR. An investigation of the antitumor activity of *Sesbania drummondii*. J Nat Prod 1981;44:86–90. [PubMed: 7217949]

FIGURE 1A

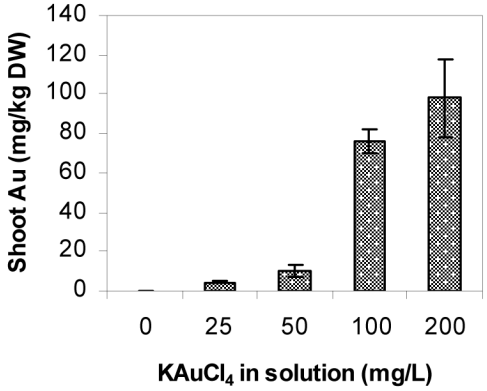

FIGURE 1B

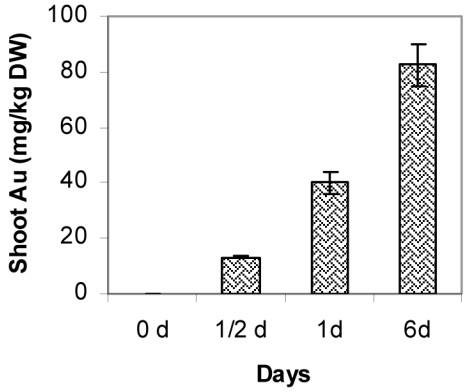

Figure 1.

A. Gold concentration in shoot (mg.Kg^{-1} DW) in *S. drummondii* grown in deionized water containing 0–200 mg.L^{-1} potassium tetrachloroaurate for 6 days. **B.** Gold concentration in shoot (mg.Kg^{-1} DW) in *S. drummondii* grown in 100 mg.L^{-1} potassium tetrachloroaurate for 0–6 days. Values are the mean of four replicates ± standard error of the mean.

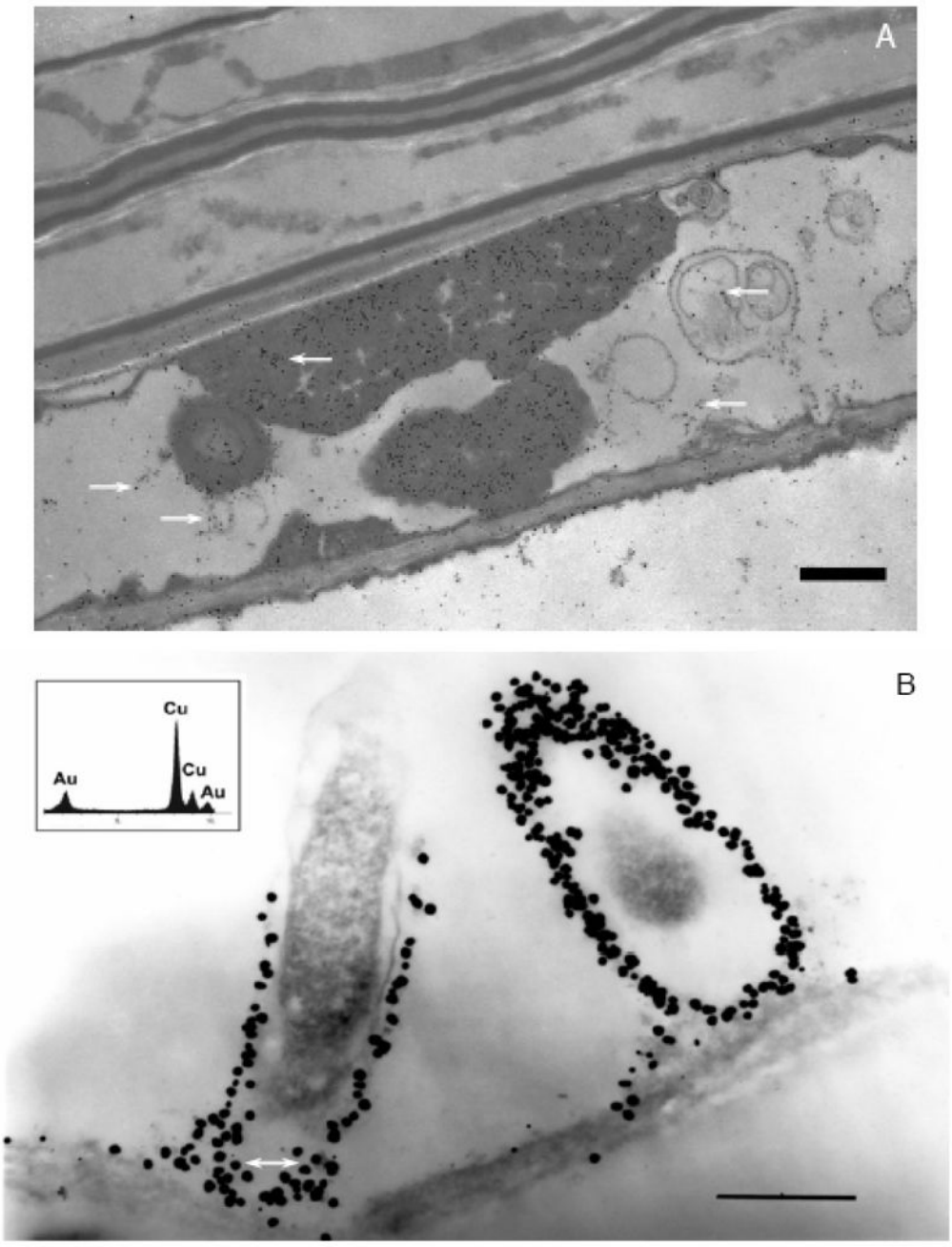

Figure 2.

A. Transmission electron microscopy of *Sesbania drummondii* root cells loaded with gold nanoparticles (magnification = 20,000X; scale marker = 1.0 μm). **B.** Transmission electron microscopy of *Sesbania drummondii* root showing numerous gold nanoparticles surrounding organelles (magnification = 60,000X; scale marker = 500 nm). The inset on the top left shows energy-dispersive spectroscopic spectrum with gold and copper peaks (copper peaks arise from the copper grid that holds the plant tissue).

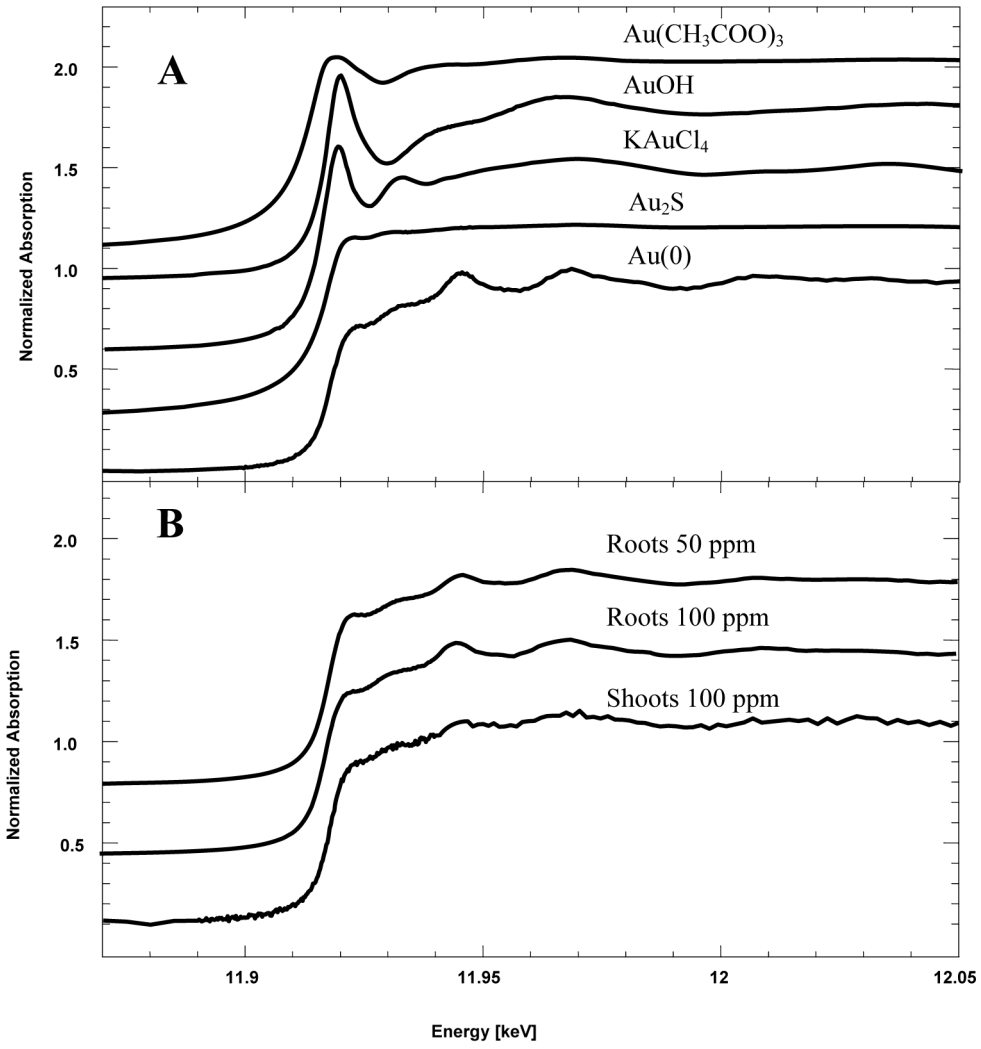

Figure 3.
A. X-ray absorption near edge structure (XANES) of gold model compounds: gold acetate, gold hydroxide, potassium tetrachloroaurate, gold sulfide, and gold metal. **B.** XANES of gold-laden plant samples.

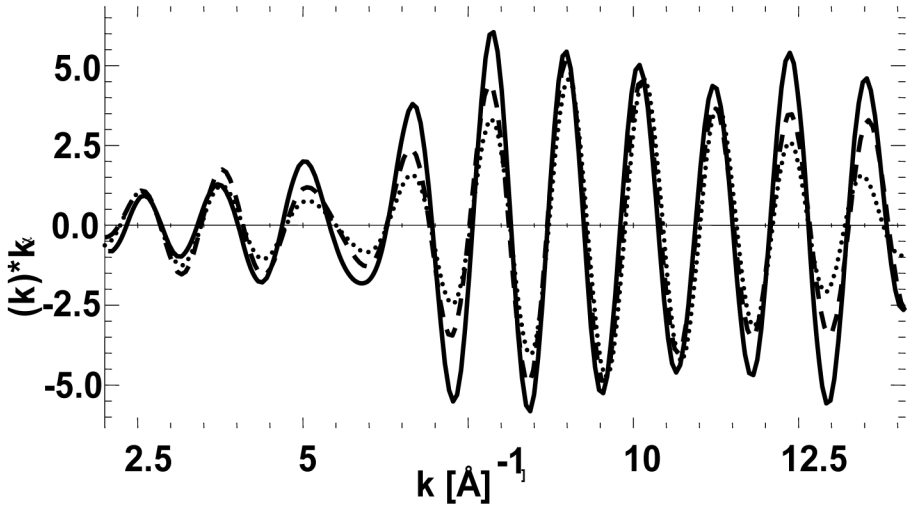

Figure 4.
Back transformed first shell Extended X-ray absorption fine structure (EXAFS) of bulk gold (solid line), gold accumulated in the root at 50 ppm (dotted line) and at 100 ppm (dashed line).

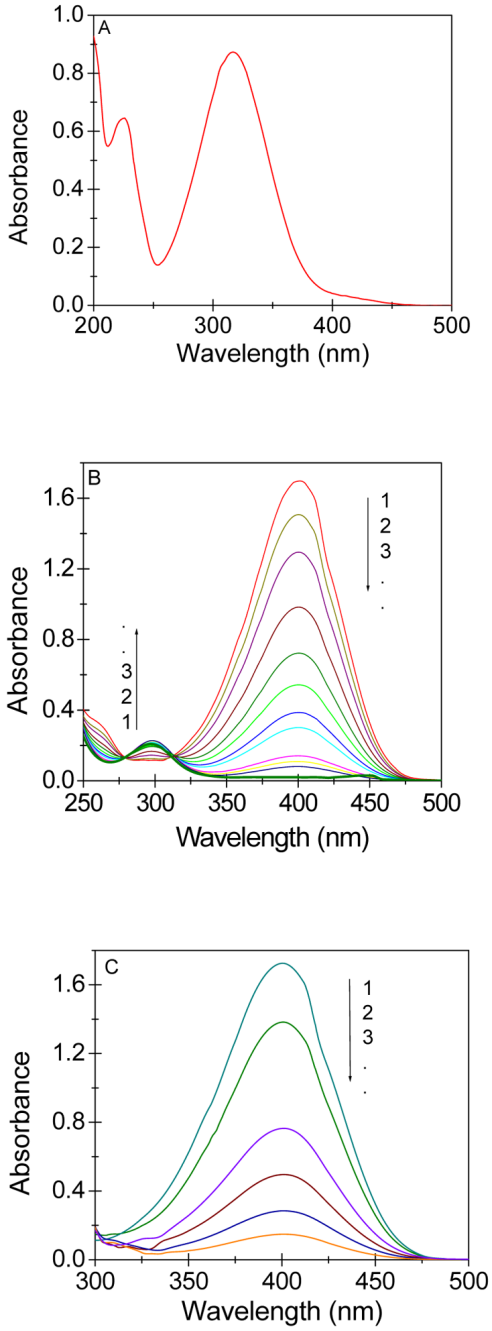

Figure 5.

A. UV-visible absorption spectra of 4-NP in aqueous solution. **B.** UV-visible absorption spectra during the successive reduction of 4-nitrophenolate ions by gold nanoparticle-rich biomatrix at an interval of 4hr. (Conditions: [Au] = 5.0×10^{-6} mol dm^{-3}, [4NP] = 6.0×10^{-5} mol dm^{-3}, [$NaBH_4$] = 3.0×10^{-2} mol dm^{-3}). **C**. UV-visible absorption spectra during the successive reduction of 4-nitrophenolate ions by the biomatrix devoid of gold. (Conditions: [4-nitrophenol] = 0.1 and [$NaBH_4$] = 15 mmol dm^{-3}).

Table 1

Growth of seedlings in different media after 6 days

Gold in media (mg/L)	Shoot (cm)	Root (cm)
Control (0)	2.9[a]	1.7[a]
25	3.0[a]	1.5[a]
50	3.3[b]	1.8[a]
100	2.9[a]	1.8[a]
200	1.0[c]	0.9[b]

Values are the mean of 4 replicates and, within each column, those not followed by the same letter are significantly different ($P<0.05$)

Table 2

LC-XANES fittings of gold accumulated in the plant root and shoot under different growth conditions

Sample	%$KAuCl_4$	%$Au(CH3COO)_3$	%Au_2S	%Au(0)	%AuOH
Au 50 ppm Roots	0.0	0.0	18.4	81.6	0.0
Au 100 ppm Roots	0.0	0.0	16.4	83.6	0.0
Au 100 ppm Shoots	0.0	0.0	14.2	84.4	1.4

Environ Sci Technol. Author manuscript; available in PMC 2008 August 22.

Table 3

First shell EXAFS fittings of gold metal and the gold present in plant tissue under different growth conditions

Sample	Interaction	CN	R(Å)	σ^2(Å^2)	S_0^2	Radius (ηm)
Gold Metal	Au-Au	12.0	2.86	0.0075	0.84	N/A
Roots 50 ppm	Au-Au	8.6	2.85	0.0081	0.84	7.6
Roots 100 ppm	Au-Au	9.8	2.85	0.0077	0.84	11.7

CN denotes the coordination number, R is the interatomic distance given in angstrom, σ^2 is the Debye Waller factor in square of angstrom, and S_0 denotes goodness of fit.